Formation and Adsorbate Interactions of Paramagnetic Pd(I) Species in Pd(II)-Exchanged NaK- and H-Clinoptilolite

Hosun Choo, A. M. Prakash, Zhidong Zhu, and Larry Kevan*

Department of Chemistry, University of Houston, Houston, Texas 77204-5641

Received: November 5, 1999; In Final Form: February 8, 2000

The formation of monovalent palladium in PdNaK-clinoptilolite where Pd(II) is introduced into extraframework sites as $[Pd(NH_3)_4]^{2+}$ by liquid-state ion exchange at 298 K, is compared to that observed in PdH-clinoptilolite where Pd(II) is incorporated by solid-state ion exchange at 823 K, using electron spin resonance (ESR) and electron spin−echo modulation (ESEM) spectroscopies. Dehydration at 473 K produces one Pd(I) species in PdH-clinoptilolite but no ESR signal in PdNaK-clinoptilolite. This indicates that the stability of Pd(I) between PdH-clinoptilolite and PdNaK-clinoptilolite is different, probably due to the different locations and environments of Pd in these systems. Hydrogen reduction of Pd(II) in these two materials after activation reveals that Pd(II) ions in PdNaK-clinoptilolite occupy relatively accessible sites in comparison to those in PdH-clinoptilolite. The interactions of Pd(I) formed by thermal reduction of PdH-clinoptilolite with various adsorbates are also studied. The ESR studies coupled with ESEM measurements show that Pd(I) in PdH-clinoptilolite interacts rapidly with molecules smaller than methanol, such as hydrogen, water, ammonia, and carbon monoxide, and forms a stable complex with them. However, adsorption of benzene and pyridine on thermally reduced PdH-clinoptilolite produces no ESR signal due to a Pd(I)−benzene complex or a Pd(I)−pyridine complex, suggesting that Pd(I) is located at a site in eight-ring channels where benzene and pyridine are too big to enter.

Introduction

It is known that zeolite-supported Pd(I) catalysts are active for various reactions such as hydrogenation,[1,2] the dimerization of small olefins,[3,4] and hydrocarbon conversion.[5,6] Their catalytic properties are strongly dependent on the nature and location of the metal ions and on their accessibility to and coordination with adsorbate molecules.[7] Therefore, the principal methods that have been used so far to study the reactivity of zeolite-supported catalysts are based on the adsorption of some typical probe molecules and their interaction with active sites. Pd(II) ions have been incorporated into extraframework sites in zeolites and other molecular sieves by liquid-phase and solid-state ion exchange,[8,9] whereas substitution of Pd(II) into framework sites of zeolites has not been reported so far. The most common oxidation states of palladium species showing paramagnetic properties are Pd(I) and Pd(III). Depending on the sample pretreatment, both paramagnetic Pd(I) and Pd(III) can be stabilized in zeolites with a relatively high negative framework charge such as in X and Y zeolites.[8,10] However, only monovalent palladium ions are generated in silicoaluminophosphate (SAPO) molecular sieves, probably due to the lower negative charge of the framework.[9,11,12]

Clinoptilolite is the most abundant natural zeolite. The framework of clinoptilolite, composed of tetrahedrally coordinated silicon and aluminum, forms a two-dimensional channel system.[13−15] Clinoptilolite is an interesting candidate for several catalytic reactions, since natural clinoptilolite is stable at relatively high temperature[16] and contains various cations to balance the negative charge of the clinoptilolite framework. Nevertheless, few studies have been done on clinoptilolite containing transition metals, mainly due to difficulties in the synthesis of clinoptilolite. Impurities such as paramagnetic Fe(III) that are commonly found in natural samples also limit the application of clinoptilolite as a catalyst as well as its characterization by ESR and ESEM spectroscopies. Recently, several papers have been reported on the synthesis of NaK-clinoptilolite without the addition of seeds,[17−19] which makes it possible to characterize clinoptilolite modified by transition metals.

In a recent work, the location of Ni(I) in synthetic clinoptilolite and its coordination with methanol, ethylene, and carbon monoxide adsorbates were studied for the first time by ESR and ESEM spectroscopies.[20] Here, we extend such studies to the palladium ion incorporated into extraframework ion-exchange sites of clinoptilolite. ESR and ESEM spectroscopies are used to monitor the formation of Pd(I) and its interaction with various adsorbates in order to provide a better understanding of active Pd(I) locations in PdH- and PdNaK-clinoptilolite.

Experimental Section

Synthesis. Single phase NaK-clinoptilolite was hydrothermally synthesized.[18] The following chemicals were used without further purification: 6 M NaOH solution, 6 M KOH solution, dried aluminum hydroxide, $Al(OH)_3$ (USP, Pfaltz & Bauer Inc.), and colloidal silica (Ludox LS, Aldrich). Synthesis was carried out in small (10 mL) stainless steel autoclaves with Teflon liners at autogenous pressure. The addition of seed crystals was important to decrease the crystallization time. The molar composition of the reaction mixture was 0.29 NaOH:1.33 KOH:1 $Al(OH)_3$:4.5 SiO_2:54.2 H_2O. In a typical synthesis, 0.87 g of dried aluminum hydroxide was added to a mixture of 0.54 mL of 6 M NaOH and 2.46 mL of 6 M KOH. After stirring the resultant mixture for 1 h, 8.26 mL of colloidal silica was added slowly and the mixture was further stirred for 1 h. Finally, 0.1 g of synthetic clinoptilolite was added as seed crystals. The final mixture was put into a static autoclave and heated at 453 K for 94 h. The final pH of the mother liquor was 9.6. After

10.1021/jp993918p CCC: $19.00
Published on Web 03/22/2000

crystallization, the product was washed with water and dried at 343 K overnight.

Pd(II)H-clinoptilolite was prepared as follows. As-synthesized NaK-clinoptilolite was ion-exchanged four times with 1 M NH_4-Cl at 333 K and calcined at 773 K in air for 24 h to obtain H−clinoptilolite where the framework negative charge is balanced by H^+. Pd(II) was incorporated into protonic clinoptilolite by solid-state ion exchange using $Pd(NH_3)_4Cl_2 \cdot H_2O$ (Alpha). A mixture of 0.08 g of palladium tetramine chloride and 1 g of H−clinoptilolite was ground in a mortar with a pestle. This solid mixture was then heated in an oven at 823 K in O_2 for 12 h and slowly cooled to room temperature. After solid-state ion exchange the color of the sample changed from white to brown. The chemical composition of this sample was $Pd_{0.021}[Al_{0.17}Si_{0.83}O_2]$ based on electron microprobe analysis. This final ion-exchanged sample is designated as PdH-Clino.

To prepare PdNa-clinoptilolite, as-synthesized NaK-clinoptilolite was ion-exchanged with 1 M NaCl solution at 343 K for 1 week. Palladium was then introduced into Na-clinoptilolite as $[Pd(NH_3)_4]^{2+}$ cation by liquid-state ion exchange with 1 mM palladium tetramine chloride (Alpha) solution at 333 K for 24 h. Before and after ion-exchange, the sample remained white. The chemical composition of this sample was $Pd_{0.005}Na_{0.036}K_{0.012}[Al_{0.17}Si_{0.83}O_2]$ based on electron microprobe analysis. Note that significant amounts of potassium ions were still present in the sample even after prolonged ion-exchange with 1 M NaCl solution. This final ion-exchanged sample is designated as PdNaK-Clino.

Sample Treatment and Measurement. Hydrated samples were loaded into 3 mm o.d. by 2 mm i.d. Suprasil quartz tubes which were evacuated overnight and sealed. The most common and most stable oxidation state of Pd is Pd(II), which is not paramagnetic. One of our goals is to find the optimum condition under which paramagnetic Pd(I) is generated with maximum ESR intensity. To prevent decay of any Pd(I) formed, all ESR spectra were recorded at 77 K. To study the behavior of the palladium as a function of dehydration, the samples were slowly heated under vacuum ($<10^{-4}$ Torr) from room temperature to 373, 473, and 573 K. This procedure accomplishes thermal reduction. To study palladium(I) interactions with various adsorbates, thermally reduced samples were exposed to the room-temperature vapor pressure of D_2O (Aldrich Chemical), CH_3OD (Stohler Isotope Chemicals), benzene (Fluka), and pyridine (Cambridge Isotopes); 20 Torr of ^{12}CO (Trigas), ^{13}CO (Cambridge Isotopes), and C_2D_4 (Cambridge Isotopes); and 14 Torr of ND_3 (Stohler Isotope Chemicals). These samples with adsorbates were frozen in liquid nitrogen and sealed for ESR and ESEM measurements. For another reduction method, dehydrated samples, after the activation process, were treated with dry hydrogen or carbon monoxide at room temperature and subsequently heated to various temperatures from 298 to 573 K for various durations. The activation treatment involves heating of dehydrated samples in 500 Torr dry oxygen at 573 K for 5 h, followed by evacuation at the same temperature overnight.

The ESR spectra were recorded with a Bruker ESP 300 X-band spectrometer at 77 K. The magnetic field was calibrated with a Varian E-500 gaussmeter. The microwave frequency was measured by a Hewlett-Packard HP 5324A frequency counter. ESEM spectra were measured at 5 K with a Bruker ESP 380 pulsed ESR spectrometer. Three pulse echoes were measured by a $\pi/2-\tau-\pi/2-T-\pi/2$ pulse sequence as a function of time T to obtain a time domain spectrum. To minimize ^{27}Al and ^{29}Si modulation from framework aluminum and silicon in measurements of deuterium modulation, the τ value was fixed, depending on the magnetic field. The deuterium modulations were analyzed by a spherical approximation for powder samples in terms of N nuclei at distance R with an isotropic hyperfine coupling A_{iso}.[21] The best fit simulation of an ESEM signal is found by varying the parameters until the sum of the squared residuals is minimized.

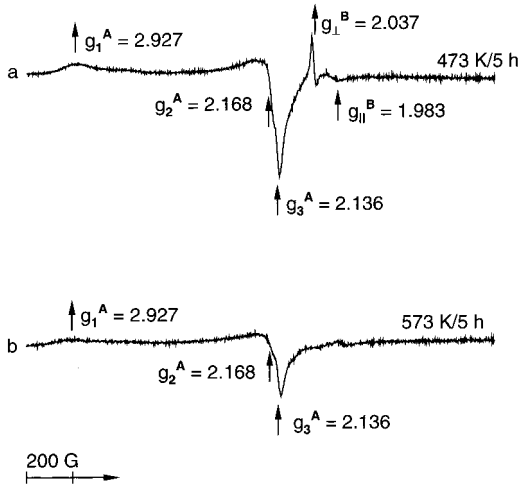

Figure 1. ESR spectra at 77 K of PdH-Clino (a) after dehydration at 473 K for 5 h and (b) after dehydration at 573 K for 5 h.

Results

ESR Measurements. Figure 1 shows the ESR spectra of thermally reduced PdH-Clino at 473 and 573 K for 5 h. Dehydration of the sample below 473 K produces no ESR signal due to Pd(I) ions formed by thermal reduction. Thus, the Pd ions exist as Pd(II). Dehydration at 473 K for 5 h generates two paramagnetic species (Figure 1a), denoted A and B. Species A with $g_1^A = 2.927$, $g_2^A = 2.168$, and $g_3^A = 2.136$ is assigned to a Pd(I) species formed by desorbing water. Species A with somewhat similar g values and axial symmetry has been reported previously in Pd(II)-exchanged H-rho ($g_\parallel = 2.713$, $g_\perp = 2.134$),[22] K−L zeolites ($g_\parallel = 2.822$, $g_\perp = 2.122$),[23] and SAPO materials ($g_\parallel = 2.919-2.895$, $g_\perp = 2.135-2.177$).[24] However, the slight rhombic symmetry of Pd(I) species A is unusual, indicating that this spectral pattern is associated with the crystal structure of clinoptilolite. Species B has axial symmetry with reversed g tensors ($g_\parallel = 1.983$ and $g_\perp = 2.037$) and has been observed in several SAPO materials ($g_\parallel = 1.988-1.983$ and $g_\perp = 2.047-2.037$)[10,25] after adsorption of dry oxygen or D_2O on an activated sample at room temperature. Upon increasing the reduction temperature to 573 K, the intensities of both species A and B are reduced (Figure 1b) and the sample color changes from brown to dark gray, suggesting that some of the Pd(I) formed is further reduced to Pd(0) at higher temperature.

Figure 2a shows the effect of oxygen adsorption on thermally reduced Pd(I)H-Clino. When 20 Torr of dry oxygen is adsorbed on a thermally reduced sample at 298 K for 3 min, the intensity of species B significantly increases while that of species A decreases. This suggests that species B arises from the interaction of Pd(I) species A with oxygen. Evacuation of oxygen at room temperature for 5 min regenerates species A and causes species B to disappear at the same time (Figure 2b). This observation further supports the hypothesis that species B is a complex with oxygen. Similar behavior with respect to evacuation has been reported previously in Pd(II)-exchanged Na-MCM-22[26] and H-rho zeolite.[22] Figure 2c shows the ESR

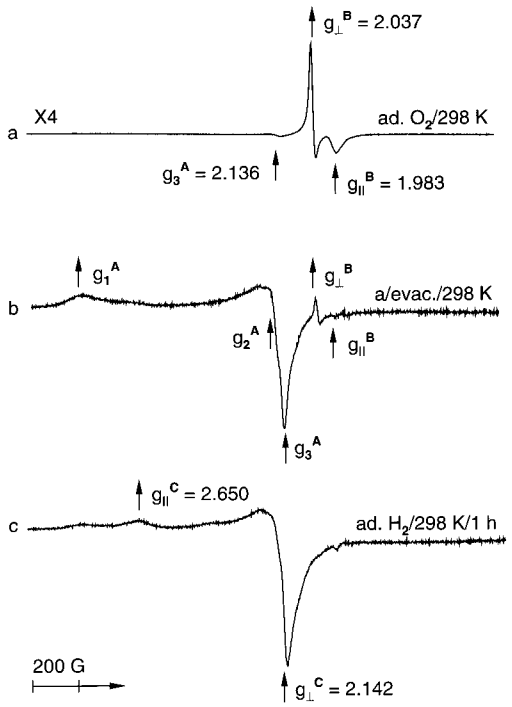

Figure 2. ESR spectra at 77 K of PdH-Clino (a) after 20 Torr of O_2 adsorption on a thermally reduced sample at 298 K for 3 min, (c) after evacuation of an O_2-treated sample at 298 K for 5 min, and (c) after 100 Torr of H_2 adsorption on a thermally reduced sample at 298 K for 0.5 h.

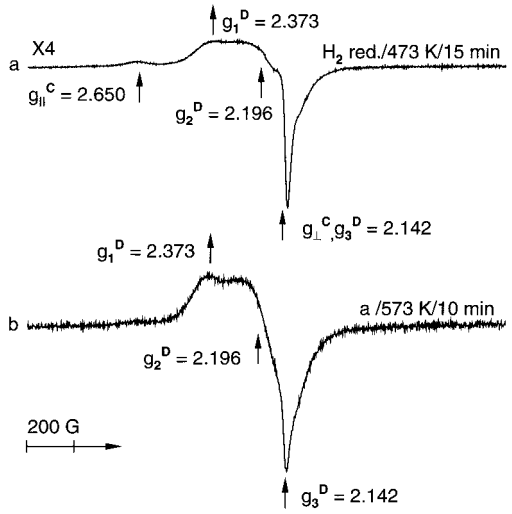

Figure 3. ESR spectra at 77 K of PdH-Clino (a) after H_2 reduction at 473 K for 15 min and (b) after H_2 reduction at 573 K for 10 min.

spectrum of PdH-Clino obtained after adsorption of dry hydrogen. When 100 Torr of dry hydrogen is exposed to thermally reduced Pd(I)H-Clino at 298 K for 30 min, species A decreases with the simultaneous appearance of a new species C. Species C has $g_{||}^C = 2.650$ and $g_\perp^C = 2.142$ and is assigned to Pd(I)$-(H_2)_n$ formed by interaction of Pd(I) species A with hydrogen since this species disappears upon evacuation of hydrogen at room temperature.

Figure 3 shows the ESR spectra of PdH-Clino after hydrogen reduction at 473 and 573 K, respectively. The sample after activation, which includes dehydration, oxidation, and evacuation, gives no ESR signal due to paramagnetic palladium species. Two species, denoted C and D, are observed when 100 Torr of dry hydrogen is adsorbed on Pd(II)H-Clino at 298 K after activation followed by subsequent heating at 473 K for 15 min. Species C is the same as already observed after hydrogen adsorption on thermally reduced Pd(I)H-Clino (Figure 2c). Species D has a rhombic g tensor with $g_1^D = 2.373$, $g_2^D = 2.196$, and $g_3^D = 2.142$. Upon increasing the temperature to 573 K (Figure 3b), species C disappears completely and only species D remains with a decrease in intensity, indicating that species C transforms to species D at high temperature and that Pd(I) ions are further reduced to Pd(0).

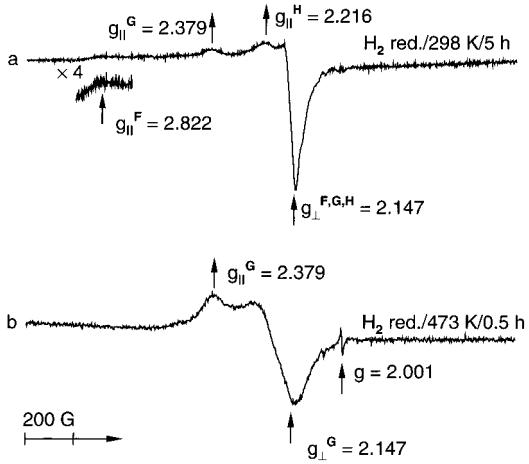

Figure 4. ESR spectra at 77 K of PdNaK-Clino (a) after adsorption of 100 Torr of H_2 on an activated sample at 298 K for 5 h and (b) after heating the above H_2-adsorbed sample at 473 K for 30 min.

Dehydration and activation of PdNaK-Clino do not generate any paramagnetic Pd(I) species, while the sample color changes from white to gray upon dehydration and to dark brown after activation. Figure 4a represents the ESR spectrum obtained after 100 Torr of dry hydrogen is exposed to activated Pd(II)NaK-Clino at room temperature for 5 h. Three axially symmetric species, denoted as F, G and H, are observed with different parallel components, $g_{||}^F = 2.822$, $g_{||}^G = 2.379$, $g_{||}^H = 2.216$, but with the same perpendicular component, $g_\perp^{F,G,H} = 2.147$. Species F has been reported in Pd(II)-exchanged K−L zeolite[23] and Y zeolites[27] and was assigned to Pd(I) species. The ESR parameters of species G are similar to those of species D produced after hydrogen reduction of PdH-Clino at high temperature, where it is assigned to a Pd(I)$-(H_2)_n$ complex. However, species H has not been observed earlier and can be assigned to another Pd(I) ion or Pd(I)$-(H_2)_n$ complex.

The reducibility of Pd(II) in PdNaK-Clino is different from that observed in PdH-Clino. In PdNaK-Clino, adsorption of hydrogen and methanol immediately reduces Pd(II) to Pd(I), even at room temperature, whereas activated Pd(II)H-Clino gives no Pd(I) ion without heating. This difference suggests that Pd(II) ions in PdNaK-Clino are located at sites more accessible to reducing agents. Figure 4b shows the ESR spectrum of PdNaK-Clino after hydrogen reduction at 473 K for 30 min. Only species G is observed without species F and H when 100 Torr of dry hydrogen is adsorbed on Pd(II)NaK-Clino at 298 K after activation with subsequent heating at 473 K for 30 min, suggesting a more favorable site for species G. Note that the ESR signal after hydrogen reduction at 473 K is very broad in comparison to that (Figure 4a) observed after hydrogen adsorption. This is probably attributable to palladium clusters formed by further reduction of Pd(I) to Pd(0). A broad isotropic ESR signal with $\Delta H_{pp} \sim 165$ has been observed at g $\sim$ 2.2 in Pd(II)-exchanged Na-MCM-22,[26] X, and Y zeolites[8,28] after heating a hydrogen-treated sample to higher temperature and in several SAPO materials[12,25] after methanol adsorption. It has

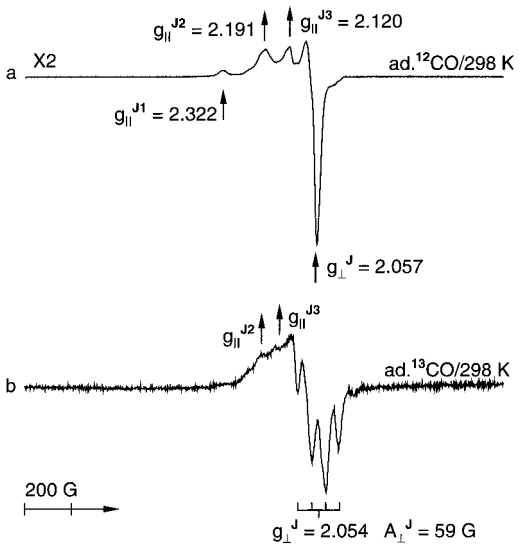

Figure 5. ESR spectra at 77 K of PdH-Clino (a) after 20 Torr of ^{12}CO adsorption and (b) after 8 Torr of ^{13}CO adsorption on a thermally reduced sample at room temperature for 30 min.

also been reported in zeolite X that temperatures higher than 500 K induce migration of Pd(0) to α-cages, where they form metal agglomerates.[8] The same broad ESR signal as in Figure 4b is also observed after adsorption of methanol on activated Pd(II)NaK-Clino at 298 K, indicating that Pd(II) is reduced to Pd(0) by methanol via an unstable Pd(I) intermediate.

The interaction of CO and Pd(I) in PdH-Clino is shown in Figure 5. When 20 Torr of ^{12}CO (^{12}C has zero nuclear spin) is adsorbed on a thermally reduced sample at 298 K for 0.5 h, species A and B disappear immediately with the formation of three new species, J_1, J_2, and J_3 (Figure 5a). These species have axial symmetry with $g_{\parallel}^{J_1} = 2.322$, $g_{\parallel}^{J_2} = 2.191$, $g_{\parallel}^{J_3} = 2.120$ and a common perpendicular component, $g_{\perp}^{J1,J2,J3} = 2.057$. When 8 Torr of ^{13}CO is added instead of ^{12}CO, the ESR spectrum (Figure 5b) shows a more complex pattern with a resolved hyperfine splitting of the $g_{\perp}$ component, $A_{\perp}$ J = 59 G. The analysis of this hyperfine structure leads to the assignment of species J to a Pd(I)−$(CO)_3$ complex.

Figure 6b,c is the ESR spectra of PdH-Clino observed after adsorption of methanol on a thermally reduced sample at room temperature for different durations. Adsorption of CH_3OD for 5 min generates a new species K with $g_{\parallel}^{K} = 2.769$ and $g_{\perp}^{K} = 2.116$ while species A still remains, indicating that only a part of Pd(I) species A is coordinated with methanol to give new species K as shown in Figure 6b. However, prolonged exposure of a sample to methanol at 298 K causes the remaining Pd(I) species A to disappear completely and produces a single species K (Figure 6c). The ESR signal due to a Pd(I)−$(CH_3OD)_n$ complex has not been reported in previous X, Y, K−L, and H-rho zeolites[8,22,23,28] or SAPO materials,[25,29] where adsorption of methanol leads to the formation of palladium clusters showing a broad isotropic ESR signal ($g = 2.070-2.14$). Formation of a Pd(I)−$(CH_3OD)_n$ complex suggests that an intermediate form, monovalent Pd(I), can be stabilized in PdH-Clino.

Figure 7a shows the ESR spectrum obtained after D_2O adsorption on thermally reduced Pd(I)H-Clino. Water adsorption produces a single species, L, with axial symmetry; $g_{\parallel}^{L} = 2.715$, $g_{\perp}^{L} = 2.127$, indicating the formation of a Pd(I)−$(D_2O)_n$ complex. Adsorption of ND_3 at room temperature on thermally reduced Pd(I)H-Clino causes Pd(I) species A to disappear completely, and simultaneously a new species M appears with $g_{\parallel}^{M} = 2.461$ and $g_{\perp}^{M} = 2.086$ (Figure 7b). An unknown

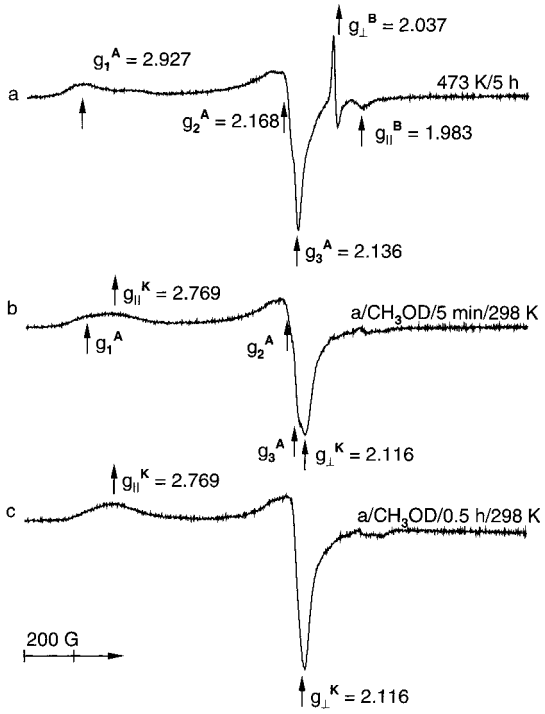

Figure 6. ESR spectra at 77 K of PdH-Clino (a) after dehydration at 473 K for 5 h, (b) after CD_3OH adsorption on a thermally reduced sample at room temperature for 5 min, and (c) after CD_3OH adsorption on a thermally reduced sample at room temperature for 30 min.

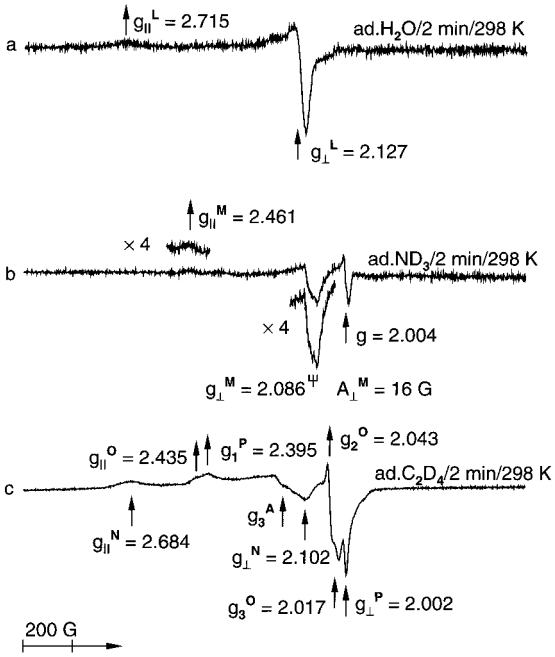

Figure 7. ESR spectra at 77 K of PdH-Clino (a) after H_2O adsorption on a thermally reduced sample at 298 K for 2 min, (b) after ND_3 adsorption on a thermally reduced sample at 298 K for 2 min, and (c) after adsorption of 20 Torr of C_2D_4 on a thermally reduced sample at 298 K for 2 min.

isotropic signal is also observed at $g = 2.00$ along with species M. Such an isotropic line in zeolites with adsorbed organic molecules is often assigned to organic free-radical formation, although the formation mechanism is unclear. The triplet feature of the perpendicular component $g_{\perp}^{M}$ results from hyperfine interaction with a ^{14}N nucleus (I = 1) and gives $A_{\perp}^{M} = 16$ G. This species M is assigned to a Pd(I)−$(ND_3)_1$ complex on the basis of hyperfine structure. It is interesting to note that, unlike

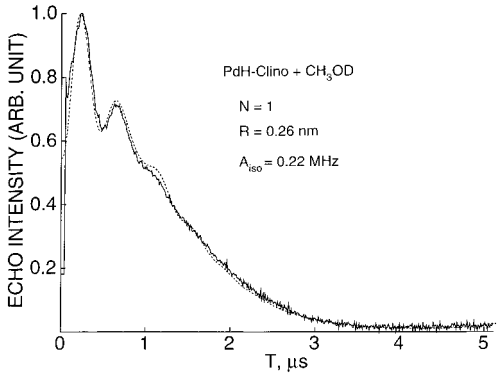

Figure 8. Experimental (—) and simulated (- - -) three-pulse ^{2}D ESEM spectra at 5 K of PdH-Clino after CH_3OD adsorption. The spectrum was recorded at the magnetic field corresponding to $g_\perp$ of species K.

TABLE 1. ESR Parameters of Pd(I) Species in PdH-Clinoptilolite Produced during Various Reduction Methods and after Adsorbate Interactions

reduction method	adsorbate	assignment	$g_{\|\|}$ or $g_\perp$	$g_\perp$ or g_2	g_3	species
thermal	none	Pd(I)	2.927	2.168	2.136	A
thermal	H_2	Pd(I)−$(H_2)_n$	2.650	2.142		C
H_2	none	Pd(I)−$(H_2)_n$	2.373	2.196	2.142	D
thermal	CH_3OD	Pd(I)−$(CH_3OD)_1$	2.769	2.116		K
thermal	CO	Pd(I)−$(CO)_3$	2.322	2.057		J_1
thermal	CO	Pd(I)−$(CO)_3$	2.191	2.057		J_2
thermal	CO	Pd(I)−$(CO)_3$	2.120	2.057		J_3
thermal	D_2O	Pd(I)−$(H_2O)_n$	2.715	2.127		L
thermal	ND_3	Pd(I)−$(ND_3)_1$	2.461	2.086		M
thermal	C_2D_4	Pd(I)−$(C_2D_4)_1$	2.684	2.102		N
thermal	C_2D_4	Pd(I)−$(C_2D_4)_1$	2.435	2.043	2.017	O
thermal	C_2D_4	Pd(I)−$(C_2D_4)_n$	2.395	2.002		P

with methanol adsorption, Pd(I) species A interacts immediately with water and ammonia to produce a single species L and M, respectively.

Figure 7c is obtained after adsorption of 20 Torr of ethylene on thermally reduced PdH-Clino at room temperature for 2 min. Several species, denoted as N, O, and P, are observed with a fraction of Pd(I) species A not interacting with ethylene. Species N and P have axial symmetry with $g_{\|}^N = 2.684$, $g_\perp^N = 2.102$, $g_{\|}^P = 2.395$ and $g_\perp^P = 2.002$ and species O is rhombic with $g_1^O = 2.435$, $g_2^O = 2.043$ and $g_3^O = 2.017$, indicating lower symmetry for species O. Species N and O are ascribed to Pd(I) complexes with ethylene based on ESEM measurements. An axial species with ESR parameters similar to those of species P has been reported earlier in several SAPO materials ($g_{\|} = 2.316-2.387$ and $g_\perp = 2.001-2.010$) and was assigned to a Pd(I)−$(C_2D_4)_n$ complex.[24,29] The intensity of Pd(I) species A decreases upon annealing an ethylene-adsorbed sample at room temperature for a longer time but still remains visible.

When benzene or pyridine is adsorbed on thermally reduced Pd(I)H-Clino, no new signal is observed, indicating that Pd(I) species A does not interact with benzene or pyridine. This suggests that Pd(I) species A is situated at a site which is inaccessible to benzene and pyridine.

Table 1 summarizes the ESR parameters assigned to the various Pd(I) species observed in PdH-Clino and PdNaK-Clino and their assignments.

ESEM Measurements. Figure 8 shows the experimental and simulated three-pulse deuterium ESEM spectra of Pd(I)H-Clino after adsorption of CH_3OD. The magnetic field is set at the value corresponding to the perpendicular component of species K (Figure 6c). The time between the first two pulses was set to 226 ns to optimize deuterium modulation. The best fit simulation shows one deuterium nucleus at a distance of 0.26 nm, indicating the formation of a Pd(I)−$(CH_3OD)_1$ complex.

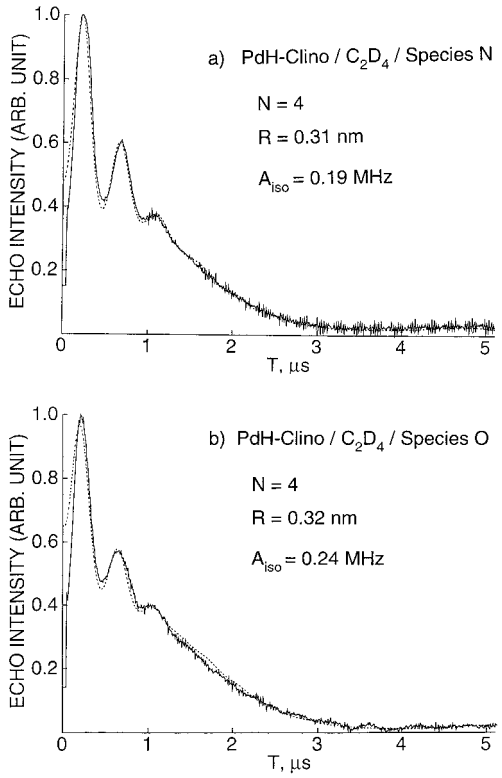

Figure 9. Experimental (—) and simulated (- - -) three-pulse ^{2}D ESEM spectra at 5 K of PdH-Clino after ethylene adsorption. The spectra were recorded at the magnetic field corresponding to (a) $g_\perp$ of species N and (b) g_3 of species O.

Parts a and b of Figure 9 respectively show the experimental and simulated deuterium ESEM spectra of Pd(I)H-Clino obtained after adsorption of C_2D_4. The spectra are recorded at a magnetic field corresponding to the perpendicular component of species N and to the g_3 component of species O, respectively (Figure 7c). The spectrum observed for species N is best simulated with four deuterium nuclei at a distance of 0.31 nm. The best fit simulation for species O indicates four equivalent deuteriums interacting with Pd(I) at 0.32 nm. These ESEM data indicate that species N and O are two Pd(I)−$(C_2D_4)_1$ complexes situated at two different sites and suggest the formation of a π-bond between Pd(I) and ethylene in both species.

Discussion

Clinoptilolite is composed of alternating SiO_4 and AlO_4 tetrahedra with a Si/Al ratio of 4.8. These units are linked together to form a two-dimensional channel structure of clinoptilolite. The 10-membered channel (A) and one eight-membered channel (B) run side by side along the *c*-axis. They are intersected by another eight-membered channel (C) that runs along the *a*-axis. Figure 10 shows the three possible cation sites in dehydrated clinoptilolite based on the cation sites identified by single-crystal X-ray diffraction in natural clinoptilolite.[15,30] Site M1 is the only cation position found in the main 10-ring channel and is close to site M3. Site M2 is located in a eight-ring channel (B) which is parallel to channel A and has a channel dimension of 0.47 nm × 0.41 nm.[31] The cations at M3 sites are coordinated to six framework oxygens at the center of channel C (channel dimension of 0.55 nm × 0.40 nm).[30]

Formation of the paramagnetic palladium species, Pd(I) and Pd(III), has been studied in several zeolites[8,22,23] and SAPO

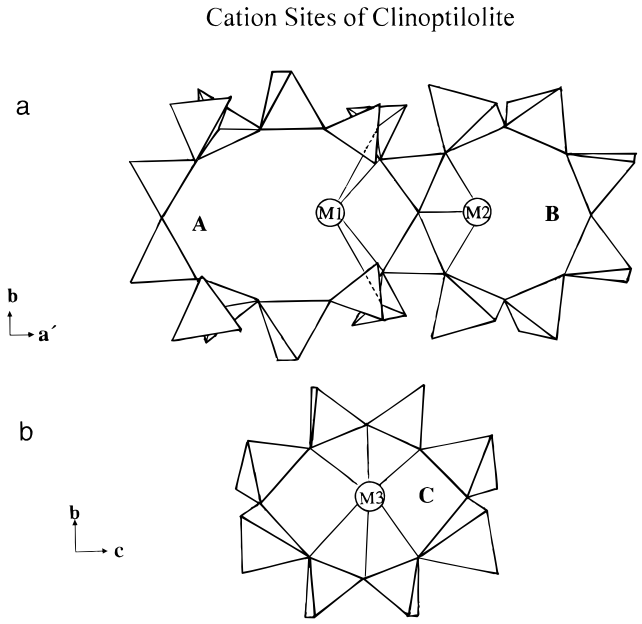

Figure 10. (a) View along the *c*-axis parallel to a 10-ring channel (A) and an eight-ring channel (B). (b) View along the *a*-axis parallel to an eight-ring channel (C). M1 to M3 represent cation locations in the clinoptilolite structure. The corners of the tetrahedra represent framework oxygens. Al and Si atoms are located at the centers of the tetrahedra. Adapted from ref 30.

materials.[24,25,29] Pd(I) species have been characterized by a rather large anisotropy of the g tensor with $g_{\|} \gg g_{\perp}$, whereas an isotropic species and a species with $g_{\|} < g_{\perp}$[32,33] have been assigned to Pd(III). Thermal reduction of PdH-Clino produces two paramagnetic species, A and B. Species A with rhombic symmetry results from the reduction of Pd(II) to Pd(I) by desorbing water. Another species, B, has been observed after adsorption of oxygen in X,Y zeolites[8,9] and SAPO materials,[10,12] where it was assigned to a Pd(II)$-O_2^-$ complex. The formation of species A and B can be explained by the following equation.

$$2\mathrm{Pd(II)} + \mathrm{H_2O} \rightarrow 2\mathrm{Pd(I)} + 2\mathrm{H^+} + {}^1/_2\mathrm{O_2}$$

The oxygen generated during the dehydration process, as shown in the above reaction, coordinates with a Pd(I) ion to give species B. This assignment is supported by the following observations. First, species B always appears with Pd(I) species A during the dehydration process and the intensities of both species decrease together as the sample is dehydrated. Second, the intensity of species B is significantly increased upon adsorption of oxygen while Pd(I) species A decreases, indicating that the oxygen interacts with Pd(I) ions. A species with reversed g values similar to that of species B has been reported in mordenite[32,33] and L zeolites,[34] where it was assigned to Pd(III) formed by oxidation of Pd(II). However, in PdH-Clino, no ESR signal due to a Pd(III) species is observed after oxidation of PdH-Clino. Therefore, species B is ascribed to a Pd(II)$-O_2^-$ complex. This species easily disappears upon evacuation of oxygen or upon adsorption of probe molecules. This indicates that oxygen is weakly bound to a palladium ion. The ESR parameters of Pd(I) species A observed in PdH-Clino show somewhat lower symmetry than those previously reported for Pd(I) in Pd(II)-exchanged SAPO materials[10,24,29] and X and Y zeolites.[8,9] Another interesting fact is, as already mentioned, the absence of Pd(III) ions after oxidation with static oxygen even at 623 K, whereas an isotropic species due to Pd(III) is observed with $g_{iso} \sim 2.23$ and $\Delta H_{pp} \sim 25$ G in zeolite X and Y (Si/Al ratios of 1.2 and 2.4).[8,9] This might be due to the low framework negative charge of clinoptilolite (Si/Al = 4.8), which is not sufficient to stabilize a higher oxidation state of palladium.

Dry hydrogen addition to thermally reduced PdH-Clino at room temperature produces only one species which is assigned to a Pd(I)$-(H_2)_n$ complex, since this species disappears upon evacuation of the hydrogen. In addition to this species, another new species with rhombic symmetry is observed as a dominant species after direct reduction of an activated sample at 473 K and is the only palladium species remaining at higher temperature. This suggests that heating a sample leads to the formation of Pd(I) at a more favorable site.

The behavior of PdNaK-Clino in the formation of Pd(I) is different from that of PdH-Clino. Unlike PdH-Clino, dehydration of Pd(II)NaK-Clino shows no ESR signal due to Pd(I) ions, indicating that Pd(I) cannot be stabilized in PdNaK-Clino. This is probably explained by different locations of Pd and different cocations in these two systems. Pd(II) ions are incorporated into these two systems by different ion-exchange methods and at very different temperatures. PdH-Clino is prepared by solid-state ion exchange at 823 K. The resultant $Pd(NH_3)_4^{2+}$ cations lose ammonia ligands and some water during the ion-exchange process,[10−12] and isolated Pd(II) ions may migrate to sites in smaller channels before dehydration. PdNaK-Clino is prepared by liquid-state ion exchange at room temperature with palladium tetramine chloride. Because of its large size (∼0.68 nm diameter), $Pd(NH_3)_4^{2+}$ is most likely located in the main 10-ring channel, where Pd(I) can be generated by thermal decomposition of $Pd(NH_3)_4^{2+}$. At the same time an unstable Pd(I) intermediate is further reduced to Pd(0). This suggestion is consistent with the observation of a broad ESR signal due to the formation of palladium clusters formed by hydrogen reduction of PdNaK-Clino at high temperature. The formation of palladium clusters seems to be associated with high temperature since such a broad ESR signal is not observed by the adsorption of hydrogen at room temperature, even after annealing overnight. Temperatures higher than 473 K cause the migration of Pd(0) to a large channel intersection where they form $(Pd(0))_n$.

The location of Pd(II) ions in $Pd(NH_3)_4^{2+}$-exchanged Na−Y zeolite has been studied by X-ray diffraction.[28] Most Pd(II) ions occupy the center of a supercage and upon increasing the temperature, $Pd(NH_3)_4^{2+}$ ion decomposes to form Pd(II), which eventually migrates toward a sodalite cage. At temperatures above 570 K most of the Pd(II) ions preferentially occupy the sodalite cage. It is also interesting to note that just room-temperature adsorption of hydrogen or methanol on activated PdNaK-Clino containing Pd(II) ions is sufficient to produce Pd(I) or Pd(0), while Pd(II)H-Clino does not generate Pd(I) without heating the sample. This indicates that the reduction of Pd(II) ions to Pd(I) ions occurs more rapidly in PdNaK-Clino than in PdH-Clino. This difference reflects that Pd(II) ions in PdNaK-Clino after the activation process occupy more accessible sites in comparison to those in PdH-Clino, which is probably due to the existence of the cocations in PdNaK-Clino.

Species J_1, J_2 and J_3, the Pd(I)-carbonyl complexes, are obtained with a common $g_{\perp}$ value after adsorption of CO on thermally reduced Pd(I)H-Clino at room temperature. The ESR spectrum observed using the 90% ^{13}C-enriched CO instead of ^{12}CO shows a hyperfine structure at $g_{\perp}$ component since ^{13}C has a nuclear spin of $^1/_2$. Four hyperfine lines of relative intensity 1:3:3:1 indicate three CO coordinating to Pd(I) ions.

Upon adsorption of methanol, only a fraction of Pd(I) species A disappears immediately to form a new species K, a Pd(I)−

$(CH_3OD)_n$ complex. The remaining species A completely interacts with methanol after annealing at room temperature for a longer time. This suggests that there are two Pd(I) species in two different environments, one being more accessible to methanol than the other. Molecules smaller than methanol, such as water, hydrogen and ammonia, interact with all the Pd(I) ions immediately. The simulation of the ^{2}D ESEM spectrum also shows that Pd(I) ion coordinates with one CH_3OD molecule at a distance of 0.26 nm. This behavior of PdH-Clino with respect to methanol adsorption is different from that observed in PdNaK-Clino, where adsorption of methanol leads to a broad ESR signal associated with the formation of palladium clusters. This difference in behavior toward methanol adsorption between PdNaK-Clino and PdH-Clino is again attributed to a difference in the location of Pd ions in the two samples. In PdNaK-Clino, Pd ions are probably situated at site M1 in the main 10-ring channel, where they can easily interact with methanol and form a palladium clusters by further reduction to Pd(0). On the other hand, the observations of a Pd(I)−(CH_3OD) complex in PdH-Clino indicates that Pd(I) is very stable toward reduction to Pd(0). This suggests that the stable Pd(I) formed in PdH-Clino is probably located at a site which is less accessible to methanol, probably at site M2 or M3 in the eight-ring channels, since migration of Pd(I) ions from these sites to the 10-ring channel is limited upon methanol adsorption, thus limiting the formation of palladium clusters.

Adsorption of water on a thermally reduced sample produces species L, a Pd(I)−$(H_2O)_n$ complex. The behavior of PdH-Clino upon adsorption of water is unusual. Water vapor usually decomposes on Pd(I) sites and forms a Pd(II)−O_2^- complex in Pd-exchanged X zeolites[8] and SAPO materials.[10,12,25] A single new species M, due to complex formation with NH_3, is observed upon adsorption of ammonia. The triplet splitting of the $g_\perp$ component indicates one NH_3 coordinating to Pd(I). The splitting and g values of this signal are very similar to that reported in PdH−SAPO-11.[29] Several species, Pd(I)−$(C_2D_4)_n$ complexes, are observed after ethylene adsorption on thermally reduced Pd(I)H-Clino. Note that Pd(I) species A formed by thermal reduction still remains visible after ethylene adsorption. This indicates that the unreacted fraction of Pd(I) is not accessible to ethylene. When ethylene is adsorbed, the part of Pd(I) species A at more accessible sites interacts immediately with ethylene and the remaining Pd(I) species A at less accessible sites more slowly coordinates with ethylene. However, the observation of an unreacted fraction of Pd(I) species A even after prolonged annealing suggests that some of the less accessible Pd(I) ions are probably blocked by large Pd(I)−ethylene complexes in eight-ring channels. ESEM data show that although both species N and O consist of one ethylene molecule coordinating to Pd(I), their simulation parameters are not the same. Thus, species N and O are assigned to two Pd(I)−(C_2D_4) complexes at different locations.

Adsorption of benzene and pyridine on thermally reduced PdH-Clino provides further information about the location of Pd(I) species A formed by thermal reduction. The fact that no new ESR signal is observed upon adsorption of benzene and pyridine indicates that Pd(I) species A does not interact with them and is located at a site not accessible to pyridine and benzene. Thus, Pd(I) ions are probably located at site M2 or site M3 in eight-ring channels B and C, respectively, since benzene and pyridine are too big to enter these eight-ring channels. However, when large polar molecules, such as pyridine, diffuse through the main 10-ring channel, cations in eight-ring channel C, which intersects the 10-ring channel, can migrate to the channel intersection and access pyridine in the 10-ring channel while cations in eight-ring channel B, which is parallel to the 10-ring channel, cannot easily access pyridine in the 10-ring channel. Thus, site M2 in eight-ring channel B seems to be the more most preferable site for Pd(I) species A in PdH-Clino.

Conclusions

ESR and ESEM spectroscopies are used to study the reducibility and adsorbate interactions of Pd(I) in PdH-clinoptilolite and PdNaK-clinoptilolite. The formation of Pd(I) in clinoptilolite is affected by the location of the Pd(II), its environment, and the cocation. Dehydration of PdH-clinoptilolite at 473 K produces a rhombic Pd(I) species formed by thermal reduction and a Pd(II)−O_2^- complex formed by the interaction of Pd(I) with oxygen, a product of dehydration. On the other hand, dehydration of PdNaK-clinoptilolite gives no ESR signal due to Pd(I). This difference can be attributed to different initial locations and types of Pd(II) in these two materials after the incorporation of Pd(II) is achieved by different ion-exchange methods at different temperatures. The high temperature during solid-state ion exchange leads to migration of Pd(II) ions to sites which are more closely coordinated to framework oxygen than those in PdNaK-clinoptilolite. Upon hydrogen reduction, the reducibility of Pd(II) in PdNaK-clinoptilolite is different from that observed in PdH-clinoptilolite. In PdNaK-clinoptilolite, hydrogen adsorption immediately reduces Pd(II) to Pd(I), even at room temperature, whereas hydrogen reduction of PdH-clinoptilolite gives no Pd(I) ion without heating the sample. This difference suggests that Pd(II) ions in PdNaK-clinoptilolite are located at sites more accessible to reducing agents and that Pd(II) is more stable in PdH-clinoptilolite than in PdNaK-clinoptilolite. This assumption is also consistent with the ESR result that adsorption of methanol on PdNaK-clinoptilolite at room temperature immediately produces a broad ESR signal due to the formation of palladium clusters in PdNaK-clinoptilolite. The ^{13}C hyperfine structure after ^{13}CO adsorption of PdH-clinoptilolite indicates that Pd(I) interacts with three CO molecules and forms a Pd(I)−$(CO)_3$ complex. Hydrogen adsorption on thermally reduced PdH-clinoptilolite at 298 K generates a single species, Pd(I)−$(H_2)_n$. Similarly, molecules smaller than methanol, such as water and ammonia, interact rapidly with Pd(I) to give the corresponding complexes, whereas adsorption of methanol on thermally reduced PdH-clinoptilolite produces a single ESR signal due to a Pd(I)−(CH_3OD) complex after prolonged annealing. Adsorption of ethylene on thermally reduced PdH-clinoptilolite shows several complexes while a small fraction of Pd(I) species A remains visible. Adsorption of pyridine and benzene on reduced PdH-clinoptilolite also shows no new ESR signal. From these various observations, we suggest that site M2 is the more preferable site for Pd(I) in PdH-clinoptilolite.

Acknowledgment. This research was supported by the National Science Foundation, the Robert A. Welch Foundation, and the Environmental Institute of Houston.

References and Notes

(1) Thomson, R. T.; Wolf, E. E. *Appl. Catal.* **1988**, *41*, 65.
(2) Thomson, R. T.; Montes, C.; Davis, M. E.; Wolf, E. E. *J. Catal.* **1990**, *124*, 401.
(3) Ghosh, A. K.; Kevan, L. *J. Phys. Chem.* **1988**, *92*, 4439.
(4) Lapidus, A. L.; Mal'tsev, V. V. *Acta Phys. Chem.* **1978**, *24*, 195.
(5) Bolton, A. P. In *Zeolite Chemistry and Catalysis*; Rabo, J. A., Ed.; American Chemistry Society: Washington, DC, 1976; Chapter 13.

(6) Chung, S. K.; Butt, J. B. *Appl. Catal.* **1990**, *64*, 173.
(7) Sachtler, W. M. H.; Zhang, Z. *Adv. Catal.* **1993**, *39*, 129.
(8) Michalik, J.; Narayama, M.; kevan, L. *J. Phys. Chem.* **1985**, *89*, 4553.
(9) Naccache, C.; Primet, M.; Mathieu, M. *Adv. Chem. Ser.* **1973**, *121*, 2661.
(10) Lee, C. W.; Yu, J. S.; Kevan, L. *J. Phys. Chem.* **1992**, *96*, 7747.
(11) Yu, J. S.; Kurshev, V.; Kevan, L. *J. Phys. Chem.* **1994**, *98*, 10225.
(12) Back, G. H.; Yu, J. S.; Kurshev, V.; Kevan, L. *J. Chem. Soc., Faraday Trans.* **1994**, *89*, 3895.
(13) Gottardi, G.; Galli, E. *Natural Zeolites*; Springer-Verlag: Berlin, 1985; p 256.
(14) Koyama, K.; Takeuchi, Y. Z. *Kristallogr.* **1997**, *145*, 216.
(15) Smyth, J. R.; Sapid, A. T. *Am. Mineral.* **1990**, *75*, 522.
(16) Kudoh, Y.; Takeuch, Y. *Mineral J.* **1983**, *11*, 392.
(17) Williams, C. D. *J. Chem. Soc., Chem. Commun.* **1997**, 2113.
(18) Zhao, D.; Szostak, R.; Kevan, L. *The Energy Lab Electronic Newsletter* **1997**, *34*, 5.
(19) Kato, M.; Satokawa, S.; Itabash, K. In *Progress in Zeolite and Microporous Materials*; Chon, H., Ihm, S. K., Uh, Y. S., Eds.; Elsevier: Amsterdam, 1997; p 717. *Stud. Surf. Sci. Catal.* **1997**, *105A*, 229.
(20) Choo, H.; Prakash, A. M.; Park, S. K.; Kevan, L. *J. Phys. Chem.* **1999**, *103*, 6193.
(21) Kevan, L. In *Time Domain Electron Spin Resonance*; Kevan, L., Schwartz, R. N., Eds.; Wiley-Interscience: New York, 1979; Chapter 8.
(22) Yu, J. S.; Kevan, L. *J. Chem. Soc., Faraday Trans.* **1995**, *91*, 3987.
(23) Yu, J. S.; Kevan, L. *Langmuir* **1995**, *11*, 1617.
(24) Hartmann, M.; kevan, L. *J. Phys. Chem.* **1996**, *100*, 4606.
(25) Yu, J. S.; Comets, J. M.; Kevan, L. *J. Phys. Chem.* **1993**, *97*, 10433.
(26) Prakash, A. M.; Wasowicz, T.; Kevan, L. *J. Phys. Chem.* **1997**, *101*, 1985.
(27) Ghosh, A. K.; Kevan, L. *J. Phys. Chem.* **1990**, *94*, 1953.
(28) Bergeret, G.; Gallezot, P.; Imelik, B. *J. Phys. Chem.* **1981**, *85*, 411.
(29) Yu, J. S.; Lee, C. W.; Kevan, L. *J. Phys. Chem.* **1994**, *98*, 5736.
(30) Armbruster, T. *Am. Mineral.* **1993**, *78*, 260
(31) Ackley, M. W.; Yang, R. T. *AIChE J.* **1991**, 1645.
(32) Shpiro, E. S.; Baeva, G. N.; Sass, A. S.; Shvets, V. A.; Fasman, A. B.; Kazanskii, V. B.; Minachev, Kh. M. *Kinet. Katal.* **1988**, *28*, 1236.
(33) Ben Tarrit, Y.; Vedrine, J. C.; Dutel, J. F.; Naccache, C. *J. Magn. Reson.* **1978**, *31*, 251.
(34) Gandhi, S. N.; Lei, G. D.; Sachtler, W. M. H. *Catal. Lett.* **1993**, *17*, 117.